LETTER

doi:10.1038/nature20817

Weak synchronization and large-scale collective oscillation in dense bacterial suspensions

Chong Chen[1]*, Song Liu[1]*, Xia-qing Shi[2], Hugues Chaté[3,4] & Yilin Wu[1]

Collective oscillatory behaviour is ubiquitous in nature[1], having a vital role in many biological processes from embryogenesis[2] and organ development[3] to pace-making in neuron networks[4]. Elucidating the mechanisms that give rise to synchronization is essential to the understanding of biological self-organization. Collective oscillations in biological multicellular systems often arise from long-range coupling mediated by diffusive chemicals[2,5–9], by electrochemical mechanisms[4,10], or by biomechanical interaction between cells and their physical environment[11]. In these examples, the phase of some oscillatory intracellular degree of freedom is synchronized. Here, in contrast, we report the discovery of a weak synchronization mechanism that does not require long-range coupling or inherent oscillation of individual cells. We find that millions of motile cells in dense bacterial suspensions can self-organize into highly robust collective oscillatory motion, while individual cells move in an erratic manner, without obvious periodic motion but with frequent, abrupt and random directional changes. So erratic are individual trajectories that uncovering the collective oscillations of our micrometre-sized cells requires individual velocities to be averaged over tens or hundreds of micrometres. On such large scales, the oscillations appear to be in phase and the mean position of cells typically describes a regular elliptic trajectory. We found that the phase of the oscillations is organized into a centimetre-scale travelling wave. We present a model of noisy self-propelled particles with strictly local interactions that accounts faithfully for our observations, suggesting that self-organized collective oscillatory motion results from spontaneous chiral and rotational symmetry breaking. These findings reveal a previously unseen type of long-range order in active matter systems (those in which energy is spent locally to produce non-random motion)[12,13]. This mechanism of collective oscillation may inspire new strategies to control the self-organization of active matter[14–18] and swarming robots[19].

Like many other flagellated bacteria, *Escherichia coli* cells can swarm over the surface of solid substrates such as agar plates[20], forming densely packed colonies with a surface packing fraction[21] of about 50%. Under standard growth conditions (see Methods), *E. coli* cells (0.8 μm in diameter, 2–4 μm in length) produce a 5–10-μm-thick layer of 'swarm fluid'[22] spanning most of the agar surface, in which they swim at a mean speed of 34 μm s^{-1} (Extended Data Fig. 1). The resulting quasi-two-dimensional dense bacterial suspension can persist over large spatial scales (centimetres) for hours. We grew about one hundred of such colonies. Approximately 12 h after inoculation, the colony has invaded the whole dish and the cells, observed in phase-contrast videos, display a disordered state with collective motion at small spatial scales (a few tens of micrometres) taking the form of transient jets and vortices (Supplementary Video 1). This 'bacterial' or 'mesoscale' turbulence has been described recently and the rheology of concentrated suspensions received a lot of attention from active matter physicists[23–26].

As the cell density increases further owing to cell multiplication (Methods), a heretofore unnoticed phenomenon emerges. Although no apparent change seems to occur in phase-contrast videos (Supplementary Video 2), their velocity, measured via particle image velocimetry (PIV) analysis (Methods) and averaged over spatial scales greater than about 100 μm undergoes regular periodic oscillations within the plane of the swarm-fluid film (Fig. 1c and Extended Data Fig. 2). This collective oscillatory motion (hereafter referred to as 'collective oscillation') is characterized by a fluctuating but featureless, spatially homogeneous velocity field that oscillates in time. (Note that this is fundamentally different from the rotational modes or vortical collective motion commonly found in biological and active matter systems under confinement[27]). Once emerged, the collective oscillation can persist for at least half an hour. The oscillation period is steady over time and ranges from 4 s to 12 s across different colonies. The orthogonal components of the collective velocity are well fitted by sinusoidal functions with identical period but different amplitude and phase (Extended Data Fig. 2), indicating that the average positions of cells follow elliptical trajectories. We observed the same collective oscillation in swarms of *Proteus mirabilis*, a species similar to *E. coli* in terms of motile behaviour but distinct in biochemistry.

The collective oscillation was also clearly manifested when we visualized the flow of the upper swarming fluid using silicone-oil droplets with minimal invasiveness (Methods). Strikingly, these tracers followed smooth and oscillatory elliptical trajectories with quasi-synchronized phases even when they were separated by hundreds of micrometres (Fig. 1b and Supplementary Video 2). Their velocity and the collective velocity of cells were in synchrony as well (Fig. 1c), suggesting that the oscillatory flow was generated by the collective motion of cells that drag nearby fluid along[28]. The amplitude of the collective velocity was somewhat smaller than that of the tracers owing to the averaging procedure.

In our experiments we found elliptical collective oscillations most often (68 out of 71 cases), with rare exceptions being linear or irregular oscillations (3 out of 71 cases; Extended Data Fig. 3). In almost all cases, the chirality and the long-axis orientation of collective oscillations are the same within a specific colony, but the chirality has an equal probability of being clockwise or counterclockwise across different colonies (Extended Data Fig. 3a), indicative of spontaneous global chiral symmetry breaking. The long-axis orientation across different colonies is non-uniformly distributed (Fig. 2a), probably reflecting the anisotropy of the large-scale geometry of colonies (Extended Data Fig. 1). These results imply that the collective oscillation of cells is correlated over very long distances. To verify this, we measured the period and phase of collective oscillations in an array of spots spanning an area of $9 \times 9\ mm^2$ (Fig. 2b) (Methods). Remarkably, the period remains nearly identical across such a macroscopic area (Fig. 2c), while the phase varies linearly over space (Fig. 2d). The collective oscillation of cells is thus organized over centimetres (more than 10^4 times the cell length) in the form of longitudinal travelling waves. In the example

[1]Department of Physics and Shenzhen Research Institute, The Chinese University of Hong Kong, Shatin, Hong Kong, China. [2]Center for Soft Condensed Matter Physics and Interdisciplinary Research, Soochow University, Suzhou 215006, China. [3]Service de Physique de l'Etat Condensé, CEA, CNRS, Université Paris-Saclay, CEA-Saclay, 91191 Gif-sur-Yvette, France. [4]Beijing Computational Science Research Center, Beijing 100094, China.
*These authors contributed equally to this work.

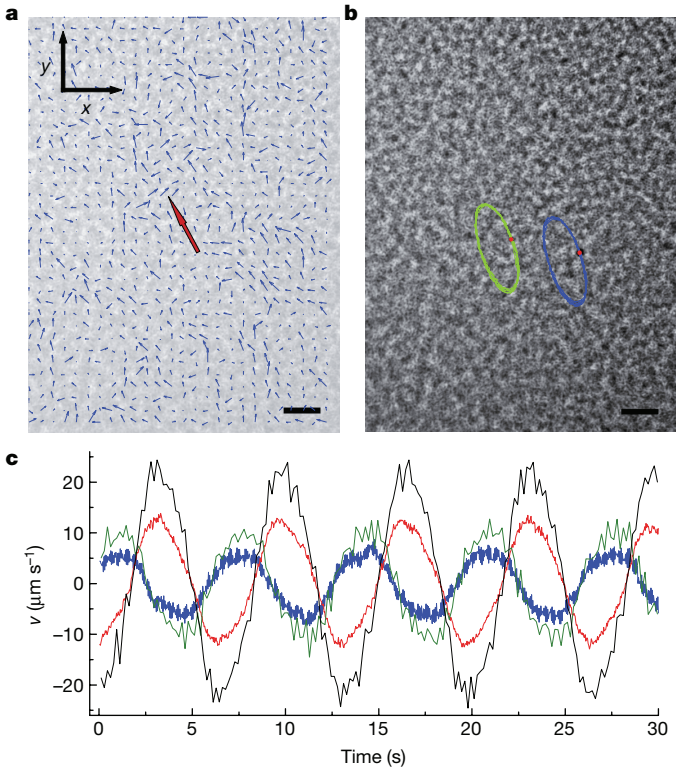

Figure 1 | Collective oscillation in dense suspensions of *E. coli*. **a**, Representative velocity field of cells' collective motion obtained by PIV analysis (see Methods). The red arrow indicates the direction of average velocity. In all experimental figures throughout the paper, the $+x$ axis represents the colony expansion direction (Extended Data Fig. 1). **b**, In the same field of view as **a**, two silicone oil tracers (red dots) displayed synchronized oscillation in elliptical trajectories (Supplementary Video 2). The background is the first frame of Supplementary Video 2. Scale bars in **a** and **b** are 20 μm. **c**, Cells' collective velocity (blue, x-axis component; red, y-axis component) and tracer velocity (green, x-axis component; black, y-axis component) in Supplementary Video 2 plotted against time.

given in Fig. 2d, the phase propagated with a wavelength of 17 mm and a phase velocity of 3.7 mm s^{-1}. Interestingly, the long axis of collective oscillations tends to be perpendicular to the propagation direction of travelling waves.

Next we examined individual trajectories of bacteria within colonies displaying collective oscillation using fluorescent cells (Methods). As suggested by phase-contrast videos (Supplementary Video 2), we found that cells moved erratically without obvious periodic motion but with frequent abrupt turns that are probably due to cell–cell collisions or flagellar switching in a dense environment (Fig. 2e and Supplementary Video 3). Cells also occasionally swam close to the surface and their motion was then weakly biased towards the chirality of the collective oscillation (Extended Data Fig. 4). Sharp turns among different cells were not synchronized, and the time interval between two consecutive turns of the same cell approximately followed an exponential distribution with an average of 2.1 ± 1.9 s (mean ± s.d., $n = 118$) (Extended Data Fig. 5). This suggests that individual cells do not behave as oscillators, and that the collective oscillation is an emergent weak synchronization phenomenon at the population level, in contrast to most other collective biological oscillations studied[2–11].

We then sought to control the emergence of the collective oscillations. We cooled down entire oscillating colonies to a temperature low enough to suppress any motion of the cells. Coming back then to the original temperature, cells started moving again with normal speed and in random directions (Methods). The collective oscillation typically re-emerged from random motion in about 30 min. At onset an irregular oscillation first emerged spontaneously, then its amplitude increased and a typical elliptic trajectory was recovered within less than one minute (Fig. 3a, c and Extended Data Fig. 6a, b). Remarkably, the long-axis orientation and the chirality were uncorrelated to the original one. These results confirm that collective oscillation is the result of spontaneous symmetry breaking. In fact, we also found that collective oscillation in cooled-off colonies may re-emerge simultaneously in several regions with different chirality and we observed that the interface separating two adjacent regions with collective oscillations of opposite chirality moves, resulting in local chirality switching accompanied by a gradual change of the orientation of the ellipses (Fig. 3b, d and Extended Data Fig. 6c, d). This observation suggests that travelling waves seen in naturally developed colonies may result from the competition of collective oscillations having emerged in different domains and are not strongly coupled with colony development.

Finally, we investigated the mechanism driving collective oscillations. We optically deactivated the motility of cells in a small area of colonies already displaying collective oscillation (Methods; Extended Data Fig. 7 and Supplementary Video 4). We found that as the speed of the cells decreased, the amplitude of collective oscillation, as measured by the collective cell velocity and by tracer velocity, decreased as well and eventually almost vanished when all cells became totally immotile, with a small-amplitude residual oscillation reflecting the incompressibility of fluids (Extended Data Fig. 7b). On the other hand, the collective oscillation remained unchanged beyond about 50 μm outside the boundary of the motility-deactivated area (Extended Data Fig. 7c, d). These results confirm that cell motility provides the driving force of collective oscillation, and that the mechanism maintaining this emergent phenomenon is local in nature and highly robust to perturbation.

We now present a mathematical model at the individual, 'particle' level that accounts for all our experimental observations. (We note that our model cannot be fully conclusive at this stage because it is based on assumptions that will need to be confirmed by a detailed study of the complex interactions between bacteria bodies, flagella, gel substrate, and the surrounding fluid.) First, in a minimalist approach, we consider identical self-propelled particles with strictly local interactions, without modelling the surrounding fluid explicitly. Second, to account for the experimental observations left unexplained, we 'immerse' this model in some Stokesian incompressible fluid.

In the Vicsek-style[16,29], 'dry' core of our model, point particles move at constant speed v_0 in a two-dimensional domain without any repulsive or attractive interaction. This allows us (1) to account for the fact that in the experimental swarming fluid layer cells can pass above each other, and (2) to simulate easily millions of cells, as required by the large-scale, high-density context of the phenomena observed. Single-particle dynamics involves an evolution equation for the velocity direction θ that allows for local alignment, but also one for the angular velocity or instantaneous frequency $\omega = \dot{\theta}$ to account for short-time memory effects introduced by the local fluid vorticity and to allow for synchronization of local rotational motion. Both these equations are stochastic, with strong noise guaranteeing erratic individual trajectories. Particles within a distance d_0 of the order of the bacteria body length are subjected to two interactions, a diffusive coupling between angular velocities of strength k_ω, and a polar alignment of strength k_θ:

$$\dot{\theta}_i = \omega_i + \frac{k_\theta}{n_i} \sum_{j\sim i} \sin(\theta_j - \theta_i) + \xi_\theta \qquad (1)$$

$$\dot{\omega}_i = -\frac{\omega_i}{\tau} + \frac{k_\omega}{n_i} \sum_{j\sim i} (\omega_j - \omega_i) + \xi_\omega + \xi_{\text{bias}} \qquad (2)$$

where the sums are over the n_i particles j currently in the neighbourhood of i, and the delta-correlated noises ξ_θ and ξ_ω are drawn from symmetric uniform distributions in the intervals $[-\eta_\theta, \eta_\theta]$ and $[-\eta_\omega, \eta_\omega]$. On the other hand, ξ_{bias} has the (current) sign of ω and its

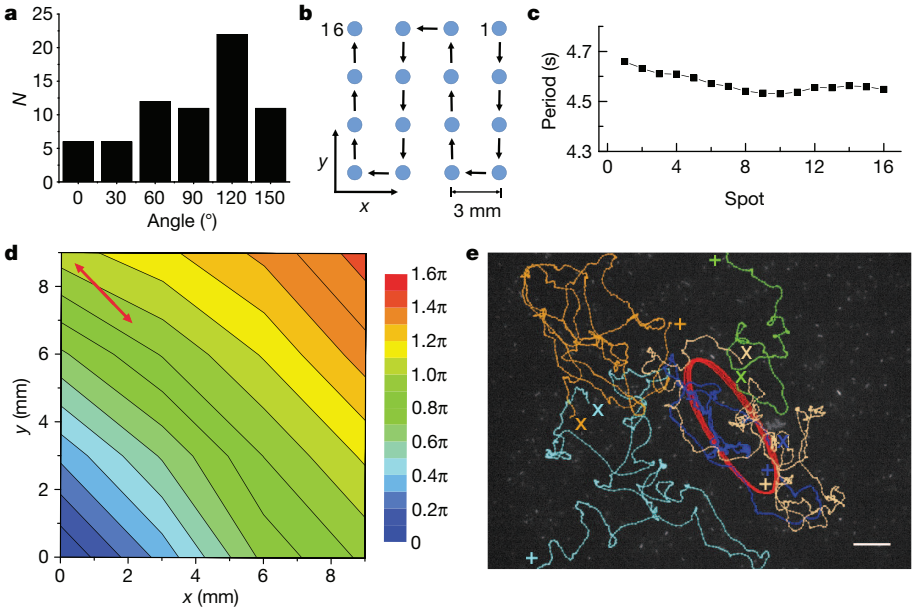

Figure 2 | Collective oscillation organized into a centimetre-scale travelling wave. a, Distribution of long-axis orientation of collective oscillations (that is, the angle defined in Extended Data Fig. 1b) across $N = 71$ colonies. **b**, Sequence of measuring a 4×4 array of spots on a colony undergoing collective oscillation (Methods). **c**, The period of collective oscillation at all spots plotted in the order of measurement. **d**, Contour map of the phase distribution of collective oscillation across the same colony as in **c**. The phase (colour scale, in radians) can be fitted as $\varphi = 0.25x + 0.27y$ (Methods), propagating at 0.37 rad mm^{-1} along its gradient direction. The double-ended red arrow indicates the long axis of collective oscillation. **e**, Single-cell trajectories in the mid-layer during collective oscillation (crosses, starting points; pluses, ending points; see Supplementary Video 3). An immotile cellular cluster (red trajectory) can serve as a flow tracer. Scale bar, 20 μm. The background is the last frame of Supplementary Video 3.

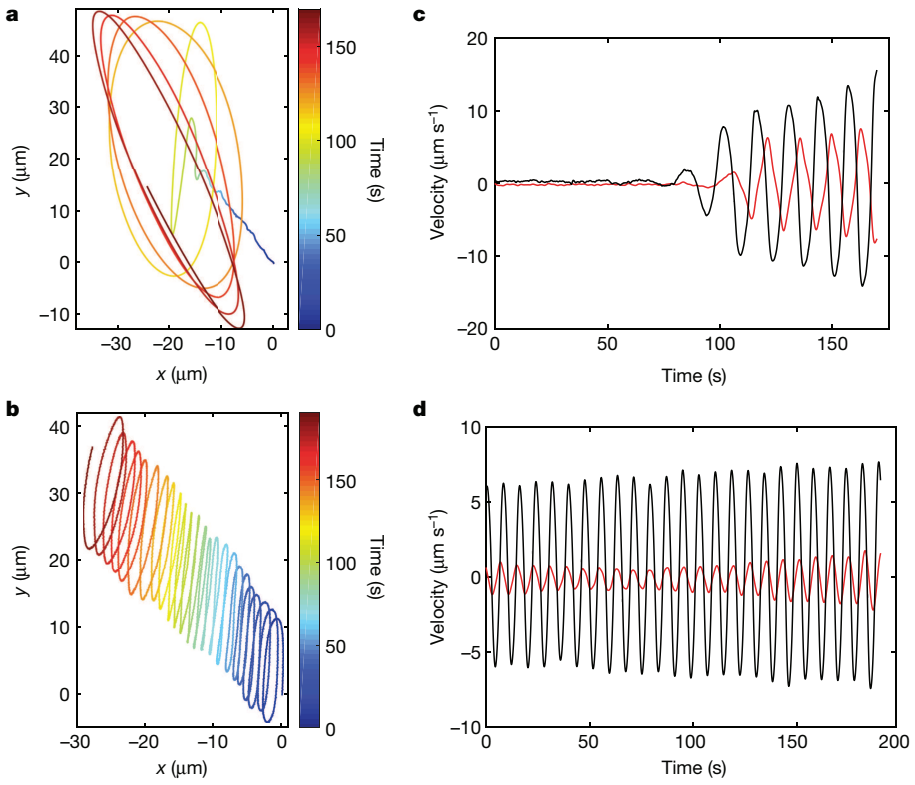

Figure 3 | Emergence of collective oscillation and chirality switching. a, Collective trajectory of cells during the emergence of collective oscillation. **b**, Chirality switching of collective oscillation from counterclockwise to clockwise during domain competition. Trajectories in **a** and **b** were built from the collective cellular velocity obtained by PIV analysis (the colour scale shows time in seconds). **c**, **d**, Collective velocities associated with **a** and **b** fitted by the smoothing spline method based on PIV data (red, x-axis component; black, y-axis component) (see Methods).

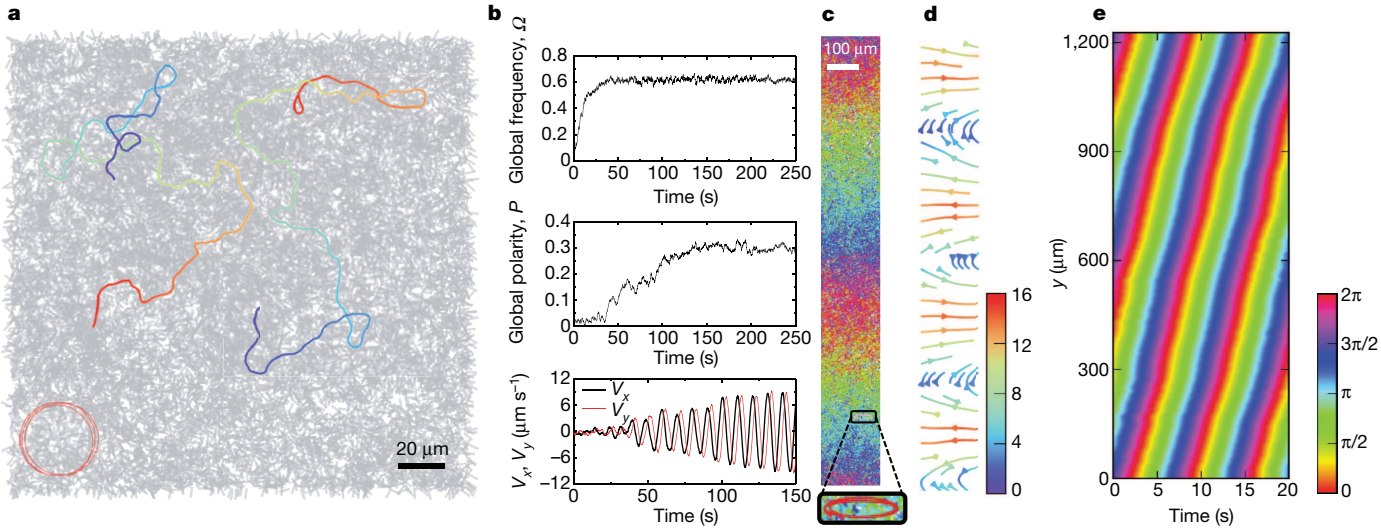

Figure 4 | Modelling results. a, Snapshot of 'dry' self-propelled particle model in a homogeneous, counterclockwise collective oscillation regime (Supplementary Video 5). Trajectories of randomly selected particles were shown during two periods of the collective oscillation cycle (start, blue; end, red). The line at the bottom left is a collective trajectory built from the averaged velocity of all particles (about 20,000). **b**, Time series of global frequency Ω, global polarity P, and collective velocity components V_x (horizontal) and V_y (vertical) from random initial conditions (same parameters as in **a**). **c**, Snapshot of the 'wet' model in a stationary travelling wave regime, with particles coloured by their orientation θ (angular colour scale on the right of **e**) (Supplementary Video 6). The inset shows the zoom of the elliptical trajectory built from the averaged velocity of particles in a 96 μm × 96 μm local domain. **d**, Fluid flow corresponding to **c** (Supplementary Video 7). The colour scale shows the intensity of the local fluid speed (in micrometres per second). **e**, Spatiotemporal dynamics of the oscillation phase of $V_x(y, t)$ showing the propagation of the travelling wave (angular colour scale).

amplitude decreases with $|\omega|$: $\xi_{\mathrm{bias}} = \mathrm{sign}(\omega_i)\exp(-|\omega_i|/\omega_0)\xi$ where ξ is a uniform noise in $[0, \eta_{\mathrm{bias}}]$. This 'bias' noise, together with the diffusive coupling between angular velocities, gives the possibility of chiral symmetry-breaking leading to a spatially homogeneous and globally oscillating velocity field. Simulations of equations (1) to (2) showed that there is a large region of parameter space where collective oscillatory motion emerges: global angular velocity $\Omega = |\langle\omega\rangle|$ and global polarity $P = |\langle\exp(i\theta)\rangle|$ take finite values while individual trajectories remain erratic (Fig. 4a, b; Methods). Not surprisingly for a diffusive oscillatory medium[30], travelling-wave configurations with arbitrary large wavelength are stable. However, as indicated by the constancy over time of Ω and P, average trajectories remain roughly circular in all cases (Fig. 4a, b), in contrast to experimental observations.

We now take into account the surrounding viscous fluid in a simplified way (see Methods for a more complete presentation). Cells interact with the surface of the agar gel, pushing themselves away from it and entraining some fluid with them. The incompressible, damped fluid is governed by a Stokes equation, creating a flow field $\boldsymbol{v}$ that advects particles: $\dot{\boldsymbol{r}}_i = \boldsymbol{v} + v_0\hat{\boldsymbol{u}}_i$ where $\hat{\boldsymbol{u}}_i$ is the unit vector of orientation θ_i. Simulations of this suspension model show that, in travelling-wave configurations, average trajectories of particles are ellipses with the long axis perpendicular to the wave propagation direction, in agreement with experimental observations (Fig. 4c–e and Fig. 2d). The model also accounts well for the residual collective oscillations seen in motility-deactivation experiments (Extended Data Fig. 8 and Supplementary Video 8).

Taking all results together, we conclude that the emergence of collective oscillatory motion in swarming flagellated bacteria is a robust self-organized process probably mediated by local interactions. A defining feature of this process is that individual cells remain strongly erratic while global order emerges. In contrast to other collective biological oscillations studied so far[2–11], which mostly arise from phase-coupling between explicit local oscillators, the phenomenon we report is characterized by two key factors. First, our system does not have 'obvious' local oscillators—they emerge only from noise upon sufficient coarse-graining; second, our synchronization is of erratic trajectories, that is, it occurs in physical space but not in phase space. As such, this phenomenon may constitute weak synchronization of stochastic trajectories, a type of ordered active matter not seen before, to our knowledge. The phenomenon may influence spatial patterning of biofilms in bacterial colonies (Extended Data Fig. 9). This mechanism of collective oscillation may be relevant to diverse biological processes that involve a large population of locally interacting cells with noisy and non-oscillating individual behaviour.

Online Content Methods, along with any additional Extended Data display items and Source Data, are available in the online version of the paper; references unique to these sections appear only in the online paper.

Received 12 June; accepted 1 November 2016.
Published online 23 January 2017.

1. Winfree, A. T. *The Geometry of Biological Time* (Springer, 1980).
2. Oates, A. C., Morelli, L. G. & Ares, S. Patterning embryos with oscillations: structure, function and dynamics of the vertebrate segmentation clock. *Development* **139,** 625–639 (2012).
3. He, L., Wang, X., Tang, H. L. & Montell, D. J. Tissue elongation requires oscillating contractions of a basal actomyosin network. *Nat. Cell Biol.* **12,** 1133–1142 (2010).
4. Herzog, E. D. Neurons and networks in daily rhythms. *Nat. Rev. Neurosci.* **8,** 790–802 (2007).
5. Muller, P. *et al.* Differential diffusivity of Nodal and Lefty underlies a reaction-diffusion patterning system. *Science* **336,** 721–724 (2012).
6. Gregor, T., Fujimoto, K., Masaki, N. & Sawai, S. The onset of collective behavior in social amoebae. *Science* **328,** 1021–1025 (2010).
7. Danino, T., Mondragon-Palomino, O., Tsimring, L. & Hasty, J. A synchronized quorum of genetic clocks. *Nature* **463,** 326–330 (2010).
8. Liu, J. *et al.* Metabolic co-dependence gives rise to collective oscillations within biofilms. *Nature* **523,** 550–554 (2015).
9. De Monte, S. *et al.* Dynamical quorum sensing: population density encoded in cellular dynamics. *Proc. Natl Acad. Sci. USA* **104,** 18377–18381 (2007).
10. Bennett, M. V. L. & Zukin, R. S. Electrical coupling and neuronal synchronization in the mammalian brain. *Neuron* **41,** 495–511 (2004).
11. Koride, S. *et al.* Mechanochemical regulation of oscillatory follicle cell dynamics in the developing *Drosophila* egg chamber. *Mol. Biol. Cell* **25,** 3709–3716 (2014).
12. Ramaswamy, S. The mechanics and statistics of active matter. *Annu. Rev. Condens. Matter Phys.* **1,** 323–345 (2010).
13. Marchetti, M. C. *et al.* Hydrodynamics of soft active matter. *Rev. Mod. Phys.* **85,** 1143–1189 (2013).
14. Nédélec, F. J., Surrey, T., Maggs, A. C. & Leibler, S. Self-organization of microtubules and motors. *Nature* **389,** 305–308 (1997).
15. Schaller, V., Weber, C., Semmrich, C., Frey, E. & Bausch, A. R. Polar patterns of driven filaments. *Nature* **467,** 73–77 (2010).

16. Sumino, Y. *et al.* Large-scale vortex lattice emerging from collectively moving microtubules. *Nature* **483,** 448–452 (2012).
17. Sanchez, T., Chen, D. T. N., DeCamp, S. J., Heymann, M. & Dogic, Z. Spontaneous motion in hierarchically assembled active matter. *Nature* **491,** 431–434 (2012).
18. Bricard, A., Caussin, J.-B., Desreumaux, N., Dauchot, O. & Bartolo, D. Emergence of macroscopic directed motion in populations of motile colloids. *Nature* **503,** 95–98 (2013).
19. Rubenstein, M., Cornejo, A. & Nagpal, R. Programmable self-assembly in a thousand-robot swarm. *Science* **345,** 795–799 (2014).
20. Kearns, D. B. A field guide to bacterial swarming motility. *Nat. Rev. Microbiol*. **8,** 634–644 (2010).
21. Darnton, N. C., Turner, L., Rojevsky, S. & Berg, H. C. Dynamics of bacterial swarming. *Biophys. J*. **98,** 2082–2090 (2010).
22. Wu, Y. & Berg, H. C. A water reservoir maintained by cell growth fuels the spreading of a bacterial swarm. *Proc. Natl Acad. Sci. USA* **109,** 4128–4133 (2012).
23. Zhang, H. P., Be'er, A., Smith, R. S., Florin, E.-L. & Swinney, H. L. Swarming dynamics in bacterial colonies. *Europhys. Lett.* **87,** 48011 (2009).
24. Sokolov, A. & Aranson, I. S. Physical properties of collective motion in suspensions of bacteria. *Phys. Rev. Lett.* **109,** 248109 (2012).
25. Wensink, H. H. *et al.* Meso-scale turbulence in living fluids. *Proc. Natl Acad. Sci. USA* **109,** 14308–14313 (2012).
26. López, H. M., Gachelin, J., Douarche, C., Auradou, H. & Clément, E. Turning bacteria suspensions into superfluids. *Phys. Rev. Lett.* **115,** 028301 (2015).
27. Lushi, E., Wioland, H. & Goldstein, R. E. Fluid flows created by swimming bacteria drive self-organization in confined suspensions. *Proc. Natl Acad. Sci. USA* **111,** 9733–9738 (2014).
28. Pushkin, D. O., Shum, H. & Yeomans, J. M. Fluid transport by individual microswimmers. *J. Fluid Mech.* **726,** 5–25 (2013).
29. Vicsek, T. *et al.* Novel type phase transition in a system of self-driven particles. *Phys. Rev. Lett.* **75,** 1226–1229 (1995).
30. Kuramoto, Y. *Chemical Oscillations, Waves, and Turbulence* (Springer, 1984).

Supplementary Information is available in the online version of the paper.

Acknowledgements We thank Y. Li and W. Zuo from our laboratory for building the microscope stage temperature control system, L. Xu (The Chinese University of Hong Kong) for providing silicone oil, H. C. Berg (Harvard University) for providing the bacterial strains, and J. Näsvall and J. Bergman (Uppsala University) for providing the mRFP plasmid. This work was supported by the Research Grants Council of Hong Kong SAR (RGC numbers 2191031 and 2130439 and CUHK Direct Grant numbers 3132738 and 3132739 to Y.W.), the National Natural Science Foundation of China (NSFC number 21473152, to Y.W.; NSFC number 11635002 to H.C. and X.S.; NSFC numbers 11474210, 11674236 and 91427302 to X.S.), and the Agence Nationale de la Recherche (project Bactterns, to H.C.).

Author Contributions Y.W. discovered the phenomenon and designed the study. C.C. and S.L. performed experiments. C.C., S.L., Y.W. analysed and interpreted the data, with input from H.C. X.S. and H.C. developed the mathematical model. All authors wrote the paper.

Author Information Reprints and permissions information is available at www.nature.com/reprints. The authors declare no competing financial interests. Readers are welcome to comment on the online version of the paper. Correspondence and requests for materials should be addressed to Y.W. (ylwu@phy.cuhk.edu.hk), H.C. (hugues.chate@cea.fr) or X.S. (xqshi@suda.edu.cn).

Reviewer Information *Nature* thanks J. Hasty and the other anonymous reviewer(s) for their contribution to the peer review of this work.